Essential Readings in Light Metals: Cast Shop for Aluminum Production.
Edited by John F. Grandfield and Dmitry G. Eskin.

Light Metals — From *Light Metals 1986*, R.E. Miller, Editor

EFFICIENCY OF INDUSTRIAL FILTERS FOR MOLTEN METAL TREATMENT
EVALUATION OF A FILTRATION PROCESS MODEL

P. Netter
Centre de Recherches
Cegedur Pechiney
38340 Voreppe France

C. Conti
Faculté Polytechnique de Mons
7000 Mons Belgique

The many practical uncertainties surrounding the evaluation of metal cleanliness make it difficult to compare the efficiencies of various liquid aluminium filtration processes. Mathematical modelling is therefore of assistance in designing deep-bed filters for molten metal, comparing their performance and monitoring their operation. This technique has been used to compare the initial performance of commercially available filter media over the velocity ranges recommended by the makers. The investigation carried out involved the preliminary characterisation of structural properties (elementary filtration cells, porosity and flow properties). Models of this type, although they may sometimes be complex, are unable to allow for the heterogeneous nature of suspensions and granular filter media, or for complex patterns of flow through these media. Data drawn from actual practical experience has to be incorporated into the model if it is to be of real utility.

INTRODUCTION

The basic principles of the filtration of aluminium alloys have long been known. This is an operation carried out to supplement treatments in the furnace (flux addition, degassing by injection lance, settling and/or the use of a degassing ladle (of the Alpur or SNIF types).

It is a process of filtration in depth (or in the bulk) whereby (Figure 1) the liquid metal flows through a porous medium designed to arrest and retain particulate matter. The filter medium may be either coherent and rigid, as in the case of the ceramic foam filter (CFF) or the rigid metal filter (RMF), or consist of a loose mass of separate particles, as in the case of the deep-bed filter (DBF).

The thickness of the filtration medium can vary (from 2 cm to 1 metre). Inclusions are retained within the bulk of the filter medium, the pores of which are big as compared to the size of the particulate matter to be removed. Nonetheless, provided the filter medium is correctly designed, the particles in suspension will lodge in the pores, by jamming between the individual grains or pores, or depositing in nooks an crannies, or by adhering to the surface of the filter medium under the effect of various transport mechanisms.

The cleanliness of the filtrate will depend on the texture of the porous medium, the form of the particulate matter to be retained an its particle size distribution, the physicochemical properties of the particulate matter and of the liquid metal, the thickness of the filter bed and rate of flow through the porous medium.

Characterisation of the metal filtering operation and the performance levels of various filters is extremely difficult by virtue of the absence of any genuinely quantitative test for assessing inclusions content in the liquid metal and/or the complications of the necessary sampling operation.

The aim of the study reported here was to improve understanding of the filtration operation via the construction of mathematical models derived from the sphere of chemical engineering. The construction of such models presupposes a satisfactory knowledge of the structural properties of the filter media. Once constructed the models make it possible to predict, for different types of inclusions, the maximum probability of contact for various filter media employed under varying operating conditions, always provided the model or models in question have first been validated experimentally.

1. FILTER MEDIA/STRUCTURAL PROPERTIES

For the filter media considered in this investigation, use can be made of the classification adopted by Apelian et al. (1) for the various porous media available for the filtration of liquid aluminium, viz :

Type 1 : Unbonded ceramic particulate
Loose ceramic media
(tabular alumina grains, alumina balls, (Alcoa type), flux grains)
Type 2 : Ceramic foams
(Conalco, Foseco and Bridgestone)
Type 3 : Bonded ceramic particulate
(TKR, Metaullics)

Within these three generic families a wide manufacturing range exists (and is reflected in differences in grain or pore sizes and in porosity).

For the purposes of this investigation, use was made of samples of those filters most representative of industrial practice.

The behaviour of the filters selected was investigated for ranges of melt velocity (rate of metal flow per unit cross-sectional area of the filter) corresponding to those recommended in the patent literature or by the makers (Table I).

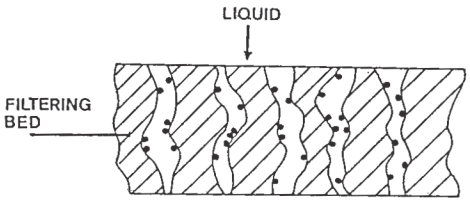

DEEP BED FILTRATION

FIGURE 1

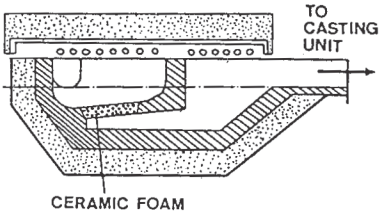

CFF TYPE PROCESS

FIGURE 2.2

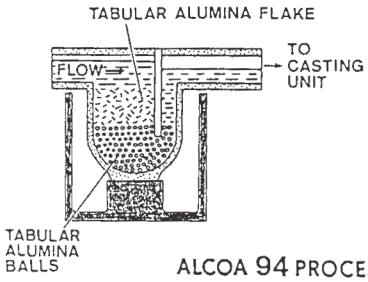

ALCOA 94 PROCESS

DEEP BED FILTER TYPE PROCESS

FIGURE 2.1

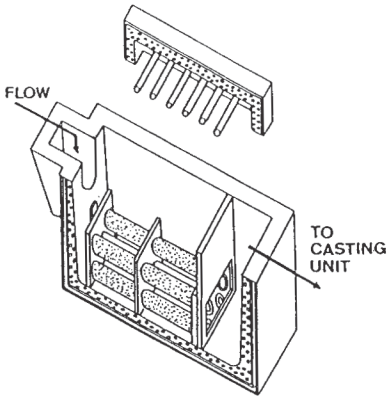

RMF TYPE BOX

FIGURE 2.3

TABLE I : FILTER MEDIA CHARACTERISTICS AND FILTRATION CONDITIONS

FILTER MEDIA CLASSIFICATION	COMMERCIAL GRADE	AVERAGE PRACTICAL GRAIN SIZE OR PORE SIZE	AVAILABLE POROSITY FOR MELT FLOW	THICKNESS	MELT APPROACH VELOCITY (cm/s)	METAL CONTACT TIME DURING FILTRATION
UNBONDED CERAMIC PARTICULATE	14 - 28 mesh	850 µm (grain)	0.40	20 cm	0.10 - 0.40	50 - 200 s
	3 - 6 mesh	2300 µm (grain)	0.39	40 cm	0.10 - 0.40	100 - 400 s
CERAMIC FOAM	40 ppi	1500 µm (pore)	0.65	5 cm	0.25 - 1.00	5 - 20 s
	30 ppi	2150 µm (pore)	0.60	5 cm	0.25 - 1.00	5 - 20 s
BONDED CERAMIC PARTICULTATE	medium grade	600 µm (pore)	0.29	2 cm	0.03 - 0.06	30 - 70 s

For each type of filter, the following grades were selected :

Type 1 : Unbonded ceramic particulate
- fine tabular medium 14 - 28 mesh
- coarse tabular medium 3 - 6 mesh

These can be employed in the Alcoa type of filtration ladle (Figure 2.1).

Type 2 : Ceramic foams
- 30 pores per linear inch
- 40 " " " "

These dimensions correspond to the commercial designations, which do not always (Conalco, Foseco) correspond to the average nombers of pores per linear centimetre which can be estimated over a cross-section of the filter medium.

Figure 2.2 illustrates the types of ladles in which they could be used

Type 3 : Bonded ceramic particulate
- 600 µm average grain diameter

Figure 2.3 outlines the use of filter cartridges.

2. DEEP-BED FILTRATION PROCESS MODELLING

2.1 Distinction between probability of contact and efficiency

The efficiency of deep-bed filtration of a suspension can be seen as the net result of two contributing factors, viz :

1) purely mechanical retention by jamming, or a sieving effect at certain preferred sites of the porous medium (2, 3)

2) local arrest on the surface of pores of the filter medium ; such retention on the surface is the end-result of two distinct processes, namely :

   - transport of particulate matter from the bulk of the suspension to the walls of the pores

   - effective retention of particulate matter on the wall under the effect of surface forces acting between the particle and the wall.

The following equation :

$$\eta_T = \eta_M + \eta_C \cdot p \qquad \text{(Eq. 1)}$$

expresses total efficiency (η_T) in terms of purely mechanical efficiency (η_M), the probability of contact between particulate matter and the wall (η_C) and the probability of retention after contact (p).

The construction of a model focussing solely on the determination of the probability of contact between particulate matter and wall (η_C) enables the retention possibilities (η_T) of a porous medium to be estimated, always provided :

- we can neglect the contribution of purely mechanical retention ($\eta_M = 0$), which is the case where the constrictions are of significantly greater size than the particles (2)

- the probability of retention after contact can be assumed to be unity, i.e. p = 1, e.g. in the case of fine inclusions in a suspension of high surface tension filtered at moderate velocity (4).

2.2 Model simulating the transport stage/assumptions made

The unit cell

Given the repetitive and periodic nature of its structure considered in the direction of flow, a porous medium can be represented as a superposition of elementary sections of height equal to the structural periodicity interval, Hc (the average diameter of grains in the case of a loose-bed filter (Figure 3)

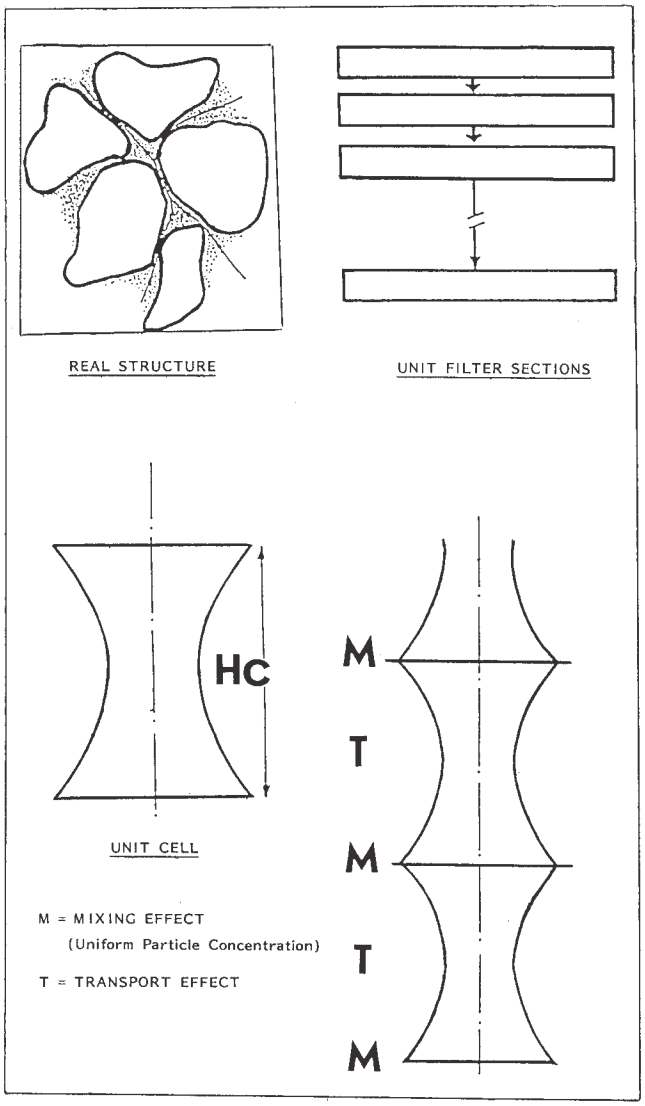

FIGURE 3

SCHEMATIC REPRESENTATION OF A GRANULAR FILTER MEDIA BY SECTIONS CONNECTED IN SERIES AND UNIT CELLS

Each of these elementary sections is considered to consist of a multiple of identical cells, the form and dimensions of which correspond to the average shape and size of the voids of the filter medium : this assumtion of a standard shape makes it possible to simulate the successive compressions and expansions undergone on average by the fluid as it passes through the reallife porous medium.

Simultaneously with the transport of the particulate matter towards the walls, the suspension undergoes a mixing action amplified by the presence of interconnections between the pores of the filter medium ; this mixing action contributes to rendering the concentration of particulate matter uniform over a cross-sectional plane normal to the direction of flow.

In order to approach the mathematics of these two phenomena, their effects have to be distinguished by supposing that they take place successively and periodically in the direction of flow ; the hypothesis generally accepted is tantamount to locating the transport phenomena within each unit cell, whereas the concentration of particulate matter is deemed to be uniform at the point of entry to each unit cell (Figures 3, 4, and 5).

The advantage of this hypothesis is that the structural periodicity interval can be made to correspond to an identical periodicity interval of standardisation of concentrations.

A general model can be proposed by considering the mixing effect to be localised both in the plane of entry to the convergent portion and in the plane of entry to the divergent portion.

Thus, a real-life filter consists of a multiple of elementary sections of height Hc/2, each corresponding to a multiple of unit cells made up of convergent and divergent portions ; Figures 4 represent the parabolic-walled unit cells for a particulate filter (Types 1 and 3) (Figure 4.1) and for a Type 2 foam filter (Figure 4.2). (The number Np of pores per sq. cm. is that which ensures that the model and the real-life filter exhibit equivalent porosities).

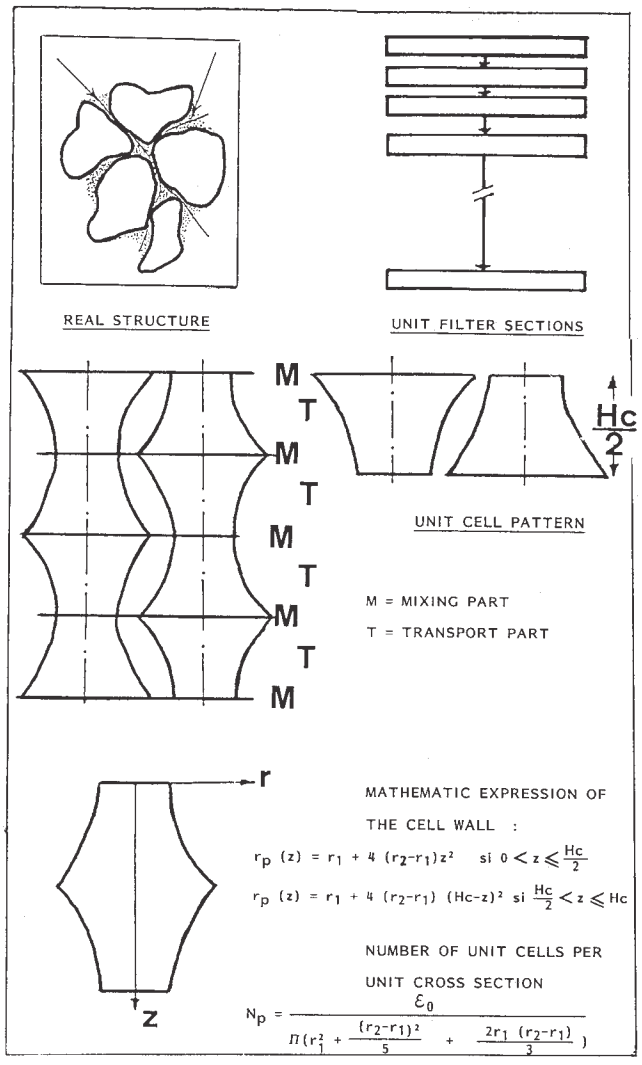

FIGURE 4.1

SCHEMATIC REPRESENTATION OF A GRANULAR FILTER MEDIA
ORIGINAL UNIT CELL PATTERN

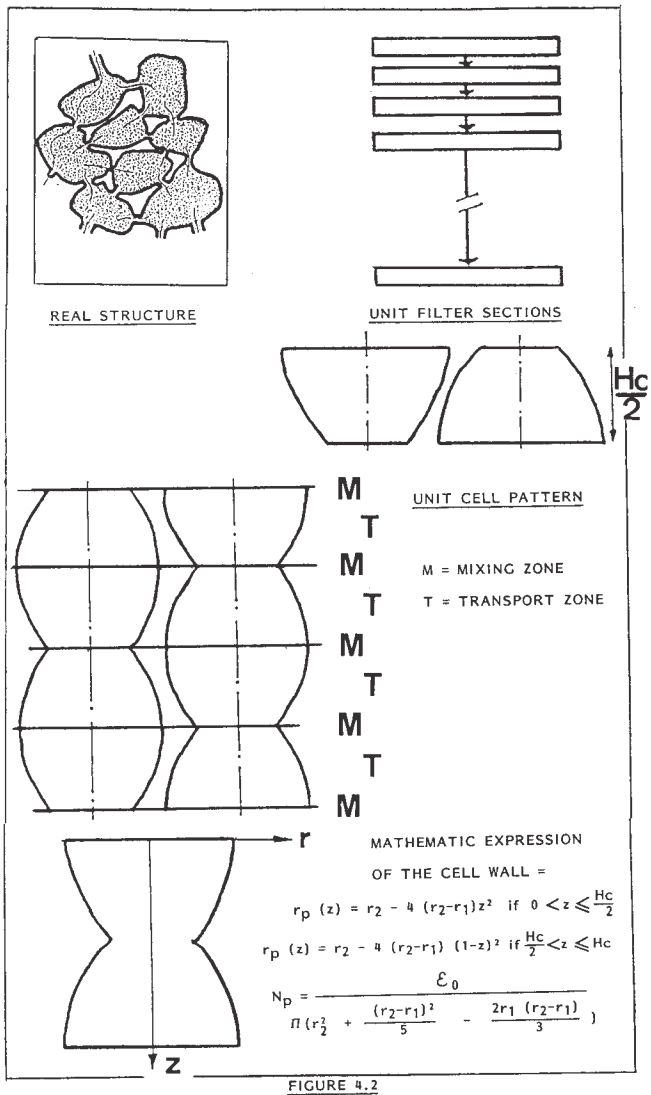

FIGURE 4.2

SCHEMATIC REPRESENTATION OF AND OPEN PORE STRUCTURE FILTER
ORIGINAL UNIT CELL PATTERN

2.3 Application of method of trajectories

Transport of the particulate matter towards the walls can be simulated by the method of trajectories, details of which are to be found in the literature (4, 5, 6, 8).

2.3.1 To this end, we require an expression for the dynamic equilibrium of a particle subjected to the forces tending to bring about sedimentation, to Van der Waals forces and to the effect of entrainment by the liquid metal.

In order to quantify the entrainment effect, it is assumed that :

- the particles are equiaxed
- the flow of the suspension through the unit cell is symmetrical about the axis and corresponds to the pattern of flow in the straight periodic tube (vertical flow).

Two limiting cases can be envisaged in order to describe the flow, viz :

1) laminar flow, which is valid for small values of Reynolds'number and, based on a simple flow pattern at the wall, affords a better physical justification of the relative importance of the effects of sedimentation and entrainment by the liquid metal.

2) flow corresponding to the actual Reynolds' number (Re) in the periodic tube, where :

$$Re = \frac{V_s \cdot H_c \cdot \rho_l}{N_p \cdot \mu} \qquad \text{(Eq. 2)}$$

(and ρ and μ are the density and dynamic viscosity, respectively, of the liquid, and V_s is the melt approach velocity), thus making it possible to determine the effect of modification of the shape of the flow lines close to the wall.

Generally speaking, the results obtained for laminar flow correspond to an upper limit on the probability of contact, since the true flow tends to render the flow lines vertical and oppose contact (4).

In a system involving a cylindrical axis (Figure 4), the differential equation for the motion of the centre of a particle is :

$$\frac{dr}{dz} = \frac{XD \sin\alpha - XN \cos\alpha}{XD \cos\alpha + XN \sin\alpha} \qquad \text{(eq.3)}$$

where :

$$XN = N_G \sin\alpha - N_S/4\delta^{+2} - A^+ (1+\delta^+)^2 F_4 \qquad \text{(eq.4)}$$

$$XD = N_G \cos\alpha F_1 + B^+(1+\delta^+) F_2 + D^+ (1+\delta^+)^2 F3 \qquad \text{(eq.5)}$$

$$N_G = \frac{2}{9} a_p^2 \frac{(\rho_p - \rho_l) g}{\mu v_s} \qquad \text{(eq.6)}$$

$$N_S = \frac{H_h}{9\pi\mu a_p^2 v_s} \qquad \delta^+ = \frac{\xi_2 - a_p}{a_p} \qquad \text{(eq.7)}$$

$$A^+ = \frac{A a_p^2}{v_s} \qquad B^+ = \frac{B a_p}{v_s} \qquad D^+ = \frac{D a_p^2}{v_s} \qquad \text{(eq.8)}$$

A, B and D correspond to the velocity $\bar{V}_f$ that the fluid would have at the position occupied by the centre of the particle if expressed by reference to its normal component ($\bar{\mu}_x$) and tangential component ($\bar{\mu}_y$), thus :

$$\bar{v}_f = - A\xi_2^2 \bar{u}_x + (B\xi_2 + D\xi_2^2) \bar{u}_y \qquad \text{(eq.9)}$$

where :

ξ_2 is the normal distance CP between the centre of the particle, C, and the point, P, on the wall

α is the angle made to the vertical by the tangent to the wall at P

ρ_p is the specific gravity of the particle

a_p is the radius of the particle

H_h is Hamaker's constant

g is the gravitational constant

F1, F2, F3 and F4 are correction factors allowing for the effect of the wall on the motion of a particle towards the wall (5).

2.3.2 The simulation calculation involves the integration of the differential equation of motion in order to determine in each part of the cell the limiting trajectory separating those particles which simply pass through it from those reaching the wall.

In the case of particulate matter of higher density than the metal, the limiting trajectories are those passing at a distance a_p from the points $A_{i+1,c}$ and $A_{i+1,d}$

In the case of particulate matter of density lower than the metal there exists in proximity to the wall a region in which the particles can move counter-current to the suspension.

In Figure 5, the positions of the points($B_{i,c}$), ($B_{i+1,c}$), ($B_{i,d}$) and ($B_{i+1,d}$) demarcating this region between the planes of entry to and exit from the unit cell are identified by determining in each of the two planes the value of r such that the denominator on the right-hand side of Equation 3 cancels out.

Therefore, if it is assumed that the particles moving counter-current reach the wall, the limiting trajectories in each such region are the trajectories passing through the points $B_{i-1,c}$ and $B_{i+1,d}$.

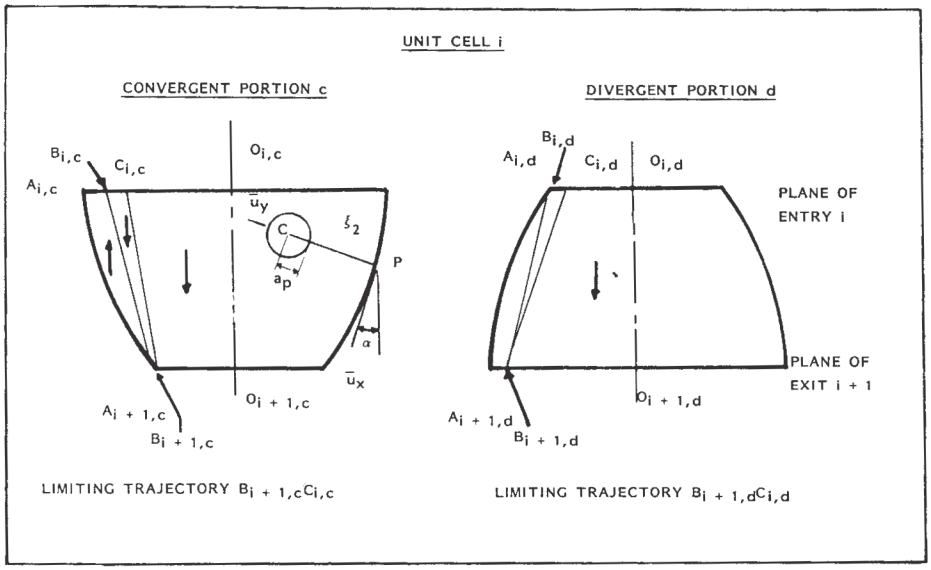

FIGURE 5

LIMITING TRAJECTORIES IN THE CONVERGENT AND DIVERGENT PORTIONS OF THE UNIT CELL (foam filter)

2.3.3 The simulation necessitates the determination of the probability of contact η_i within a unit cell as expressed by reference to the various rates of arrival, J , of particulate matter at the walls of the cell.

We have :

$$\eta_i = \frac{J_{B_{i,c}}\ C_{i,c} + J_{A_{i+1,c}}\ B_{i+1,c} + J_{B_{i,d}}\ C_{i,d} + J_{A_{i+1,d}}\ B_{i+1,d}}{J_{O_{i,c}}\ A_{i,c} + J_{O_{i,d}}\ A_{i,d}} \qquad \text{(Eq.10)}$$

These various rates of arrival can be expressed by reference to the flux function Ψ and to the concentrations C_i and C_{i+1} in the planes of entry to and exit from the unit cell.

Whence :

$$\eta_i = CU + DU + \frac{C_{i+1}}{C_i}(CL + DL) \qquad \text{(Eq.11)}$$

Where ...

$$CU = \frac{\Psi_{C_{i,c}} - \Psi_{B_{i,c}}}{2 - \Psi_{A_{i,c}} - \Psi_{A_{i,d}}} \qquad \text{(Eq.12)}$$

(refers to the contribution of the Convergent portion with particles arriving from the Upper planes).

$$DU = \frac{\Psi_{C_{i,d}} - \Psi_{B_{i,d}}}{2 - \Psi_{A_{i,c}} - \Psi_{A_{i,d}}} \qquad \text{(Eq.13)}$$

(refers to the contribution of the Divergent portion with particles arriving from the Upper plane)

$$CL = \frac{\Psi_{B_{i+1,c}} - \Psi_{A_{i+1,c}}}{2 - \Psi_{A_{i,c}} - \Psi_{A_{i,d}}} \qquad \text{(Eq.14)}$$

(refers to the contribution of the Convergent portion with particles arriving from the Lower plane)

$$DL = \frac{\Psi_{B_{i+1,d}} - \Psi_{A_{i+1,d}}}{2 - \Psi_{A_{i,c}} - \Psi_{A_{i,d}}} \qquad \text{(Eq.15)}$$

(refers to the contribution of the Divergent portion with particles arriving from the Lower plane)

Within the range of variation of parameters investigated as part of the study reported, the entrainment effect overrides the gravity effect at the plane of constriction, so that the contribution CL can be neglected.

Since :

$$\frac{C_{i+1}}{C_i} = 1 - \eta_i \qquad \text{(Eq.16)}$$

We have :

$$\eta_i = \frac{CU + DU + DL}{1 + DL} \qquad \text{(Eq.17)}$$

The coefficient of filtration, λ_i, with respect to the unit cell and hence to the total porous medium can be expressed as follows :

$$\lambda_i = \frac{2}{Hc} \ln \left(\frac{1}{1 - \eta_i}\right) \qquad \text{(Eq.18)}$$

The probability of contact η_c for a filter of height H can then be expressed as follows :

$$\eta_c = 1 - e^{-\lambda_i H} \qquad \text{(Eq.19)}$$

3. ANALYSIS OF THE PROCESS MODEL/COMPARISON WITH EXPERIMENTAL RESULTS

3.1 Using the model

For any given filter, the process model can be employed in various ways. Thus :

- for a given combination of metal an inclusions (values of D_p, ρ_p fixed), it is possible to express the variation in filtration efficiency η with melt velocity V_S
- for a given melt velocity, V_S , it is possible to evaluate filtration efficiency versus the dimension of inclusions at a given density ρ_p.
- for a given melt velocity, V_S , and given dimensions of inclusions, it is possible to determine how filtration efficiency varies with the density of inclusion.

A filtration process can be characterised in terms of :

1) the filtration coefficient, λ_i, which refers to unit thickness of the filter,

and

2) overall filtration efficiency η , which allows for practical realities.

Figure 6, which refers to an open-pore structure filter (CFF, 30 ppi) and equiaxed inclusions of 12 µm shows the relative weights of the probabilities of contact in the convergent portion (CU) and in the divergent portion (DU + DL) of the unit cell as determined by the density of particles filtered at various melt velocities V_S

Figure 6 shows that the efficiency of the convergent portions of the constrictions decreases with particle density and also shows the gradually increasing contribution of the divergent portions.

For the unit cell as a whole, the efficiency is η_i. When calculated with respect to actual filter thickness, the variation in efficiency η' parallels that of η_i

Similarly, Figure 7 illustrates how CU, DU + DL and η_i vary with melt velocity for different particle sizes.

3.2 Comparisons of predictions of the model and experimental results

Needless to say, the aluminium/titanium boride system is the easiest to employ experimentally even if some uncertainty persists as to the mean size of the TiB_2 used as synthetic inclusions. Particle size distribution was assumed to range from 2 to 6 µm and experimental points (Figures8) were compared with the efficiencies predicted by the model at 2 and 6 µm for a density of 4.5 g/cc.

Table II sets out all results relating to the experimental determination of the initial coefficient of filtration λ_i for the liquid aluminium/titanium boride system.

TABLE II : EXPERIMENTAL CONDITIONS AND RESULTS - GEOMETRIC PARAMETERS OF UNIT CELLS (microscopic examination)

PARTICLES PARAMETERS	FILTER MEDIA		FILTRATION CONDITIONS	EXPERIMENTAL RESULTS	GEOMETRIC DIMENSIONS OF THE UNIT CELL (model)			REFERENCES	FIGURES
Suspension of Ti B_2 particles in liquid aluminium	TYPE	H THICKNESS (cm) (cm)	v_s MELT APPROACH VELOCITY (cm/s)	λi INITIAL FILTRATION COEFFICIENT (cm^{-1})	r_1 (mm)	r_2 (mm)	Hc (mm)		
	CFF 30 ppi	5 - 10	0.20 - 2.00	0.008 - 0.10	0.492	0.913	2.15	4	8.1
Assumed size range : 2 - 6 µm	CFF 40 ppi	5 - 10	0.40 - 2.00	0.020 - 0.15	0.343	0.638	1.50	4	8.2
	CFF 30 ppi	5	0.10 - 1.00	0.070 - 0.26	0.492	0.913	2.15	9	8.3
	CFF 55 ppi	2.5 - 5	0.70 - 4.00	0.040 - 0.12	0.208	0.387	0.91	12	8.4
Specific gravity 4.50 g/cm³	DBF : Ø moy = 4 mm	41.7	0.04 - 0.75	0.010 - 0.09	0.720	1.720	4.00	10	8.5
	DBF : Ø moy = 2 mm	-	0.04 - 1.00	0.035 - 0.29	0.360	0.860	2.00	9	8.6
	DBF : Ø moy = 2.30mm	40	0.12 - 0.13	0.008 - 0.02	0.414	0.989	2.30	11	8.7
	DBF : Ø moy =0.85mm	20	0.12 - 0.13	0.012 - 0.04	0.153	0.366	0.85	11	8.8
	RMF : Ø moy =0.60mm	2	0.04 - 0.05	0.04 (mean value)	0.108	0.258	0.60	11	8.9

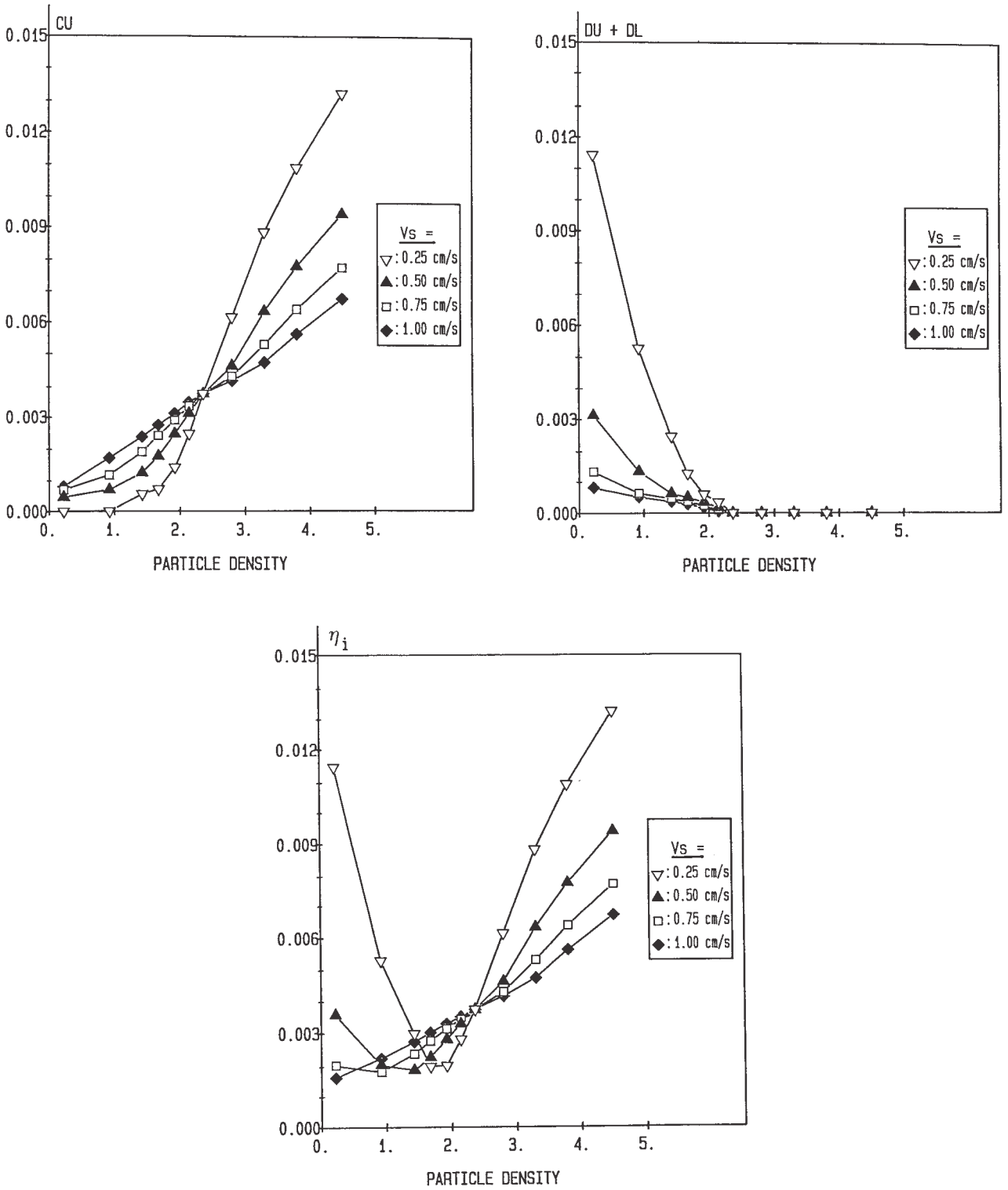

FIGURE 6

PROBABILITIES OF CONTACT IN THE CONVERGENT PORTION (CU), THE DIVERGENT PORTION (DU + DL) AND THE WHOLE OF A UNIT CELL (η_i) VERSUS PARTICLE DENSITY FOR VARIOUS MELT VELOCITIES (Vs)

(CFF, 30 ppi Hc = 2.15 mm
Region of laminar flow P_1 = 2.36
Particle diameter d_p = 12 μm)

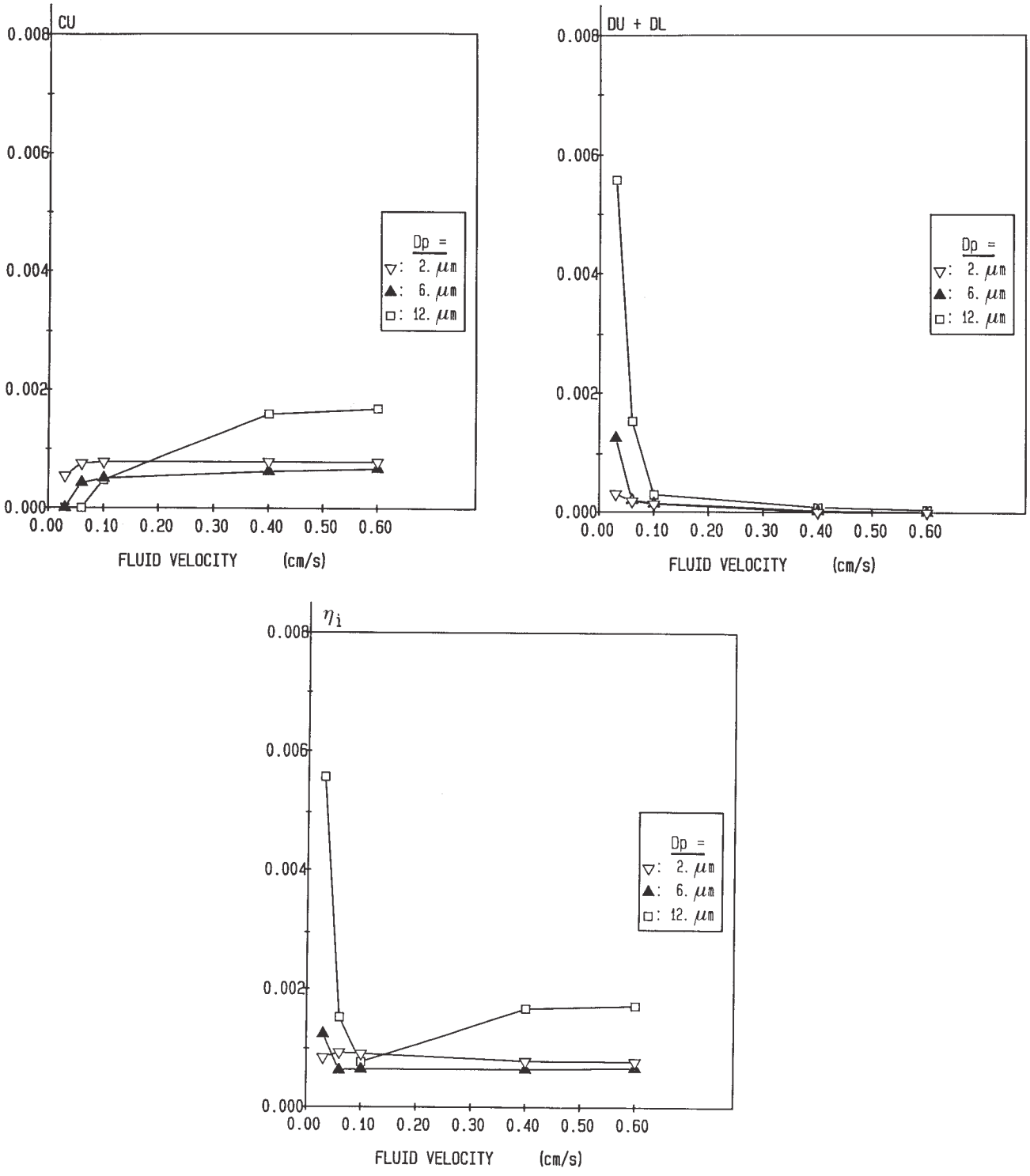

FIGURE 7

PROBABILITIES OF CONTACT IN THE CONVERGENT PORTION (CU), THE DIVERGENT PORTION (DU + DL) AND THE WHOLE OF A UNIT CELL (η_i) VERSUS MELT VELOCITY (V_s) FOR VARIOUS PARTICLE DIAMETERS (D_p)

(Fine granulate filter bed Hc = 0.85 mm
Region of laminar flow ρ_1 = 2.36 ρ_p = 2.14)

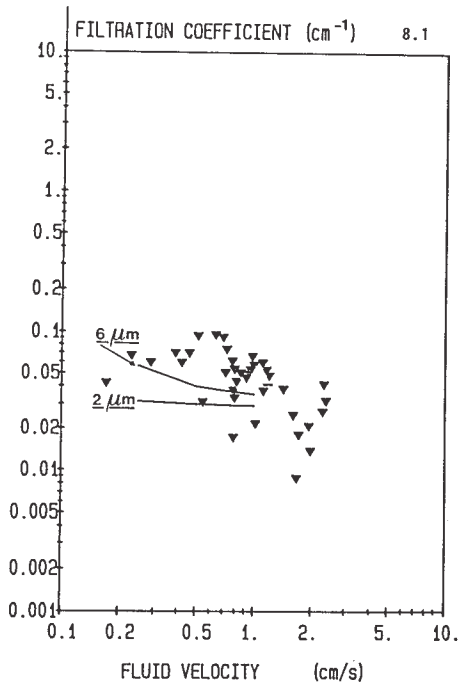

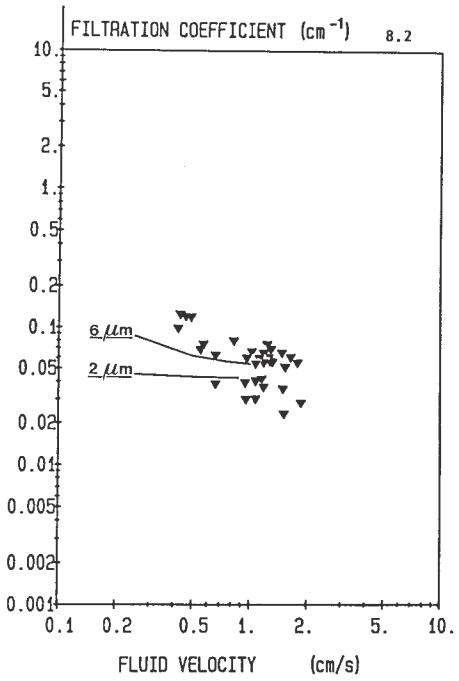

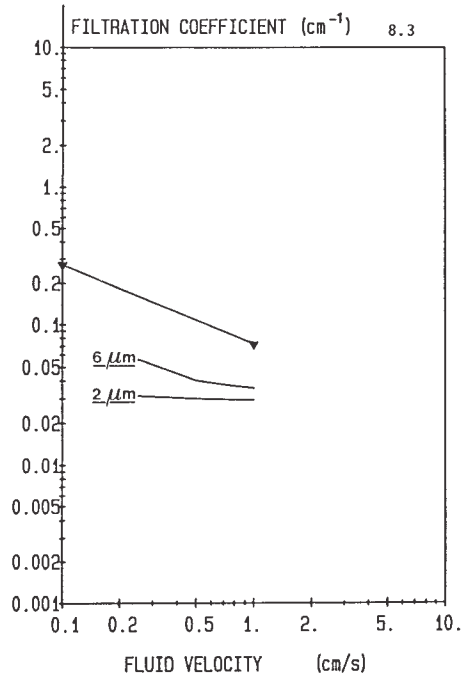

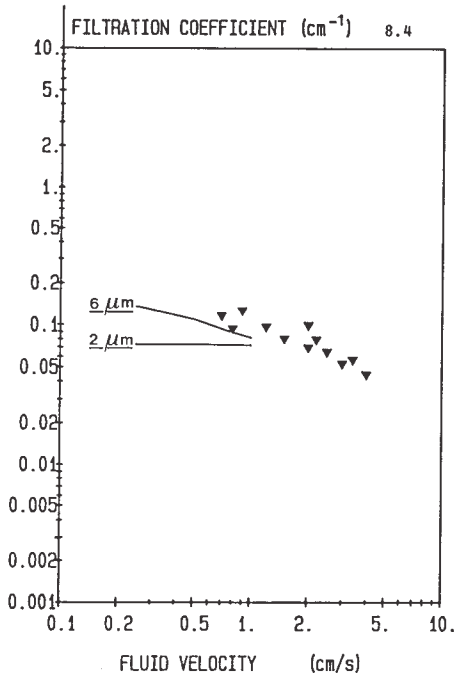

FIGURES 8.1 TO 8.4 INCLUSIVE

COMPARISON OF EXPERIMENTAL RESULTS AND CONTACT PROBABILITIES DERIVED FROM SIMULATION CALCULATIONS

Al/TiB_2 system

Type 2 filter - CFF

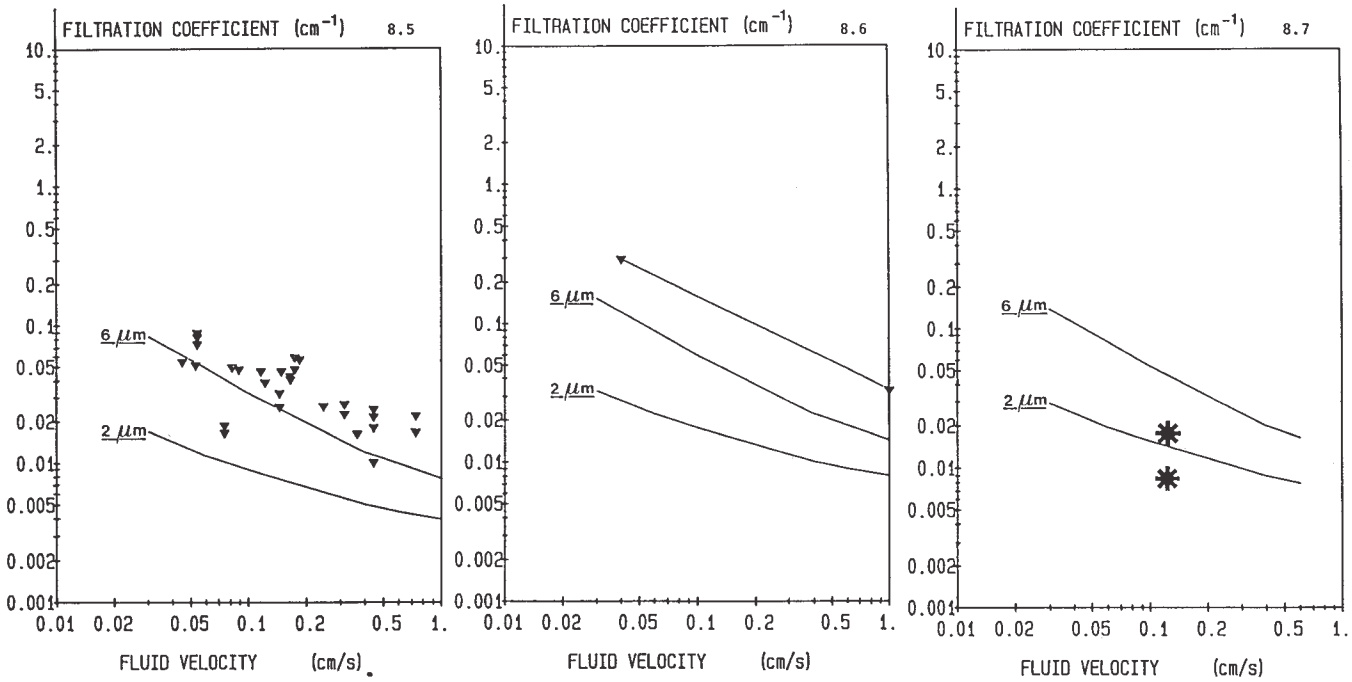

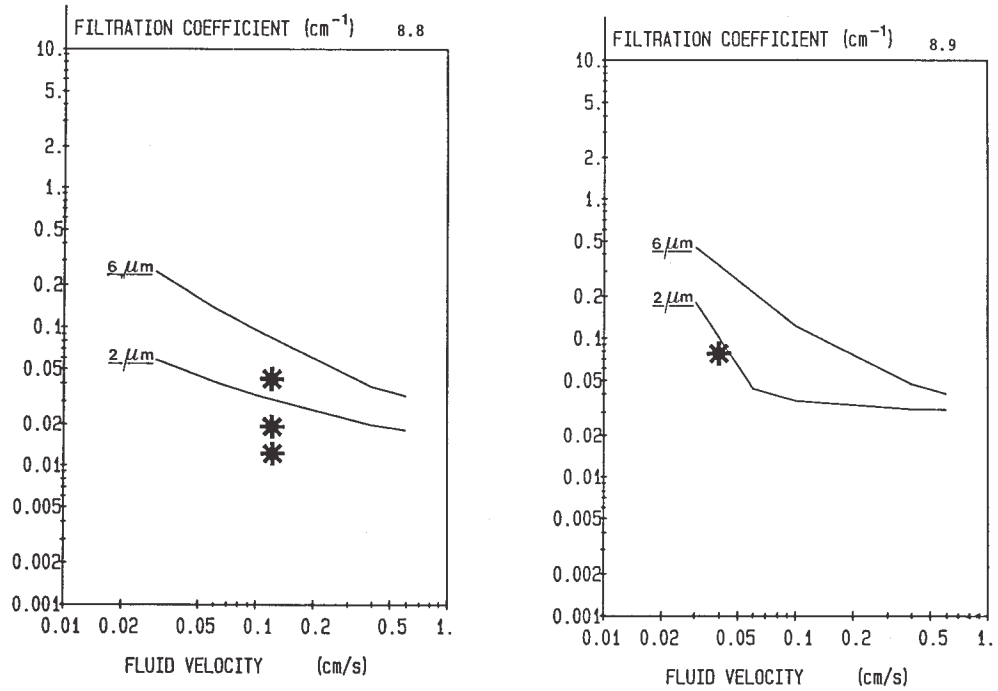

FIGURES 8.5 TO 8.9 INCLUSIVE

COMPARISON OF EXPERIMENTAL RESULTS AND CONTACT PROBABILITIES DERIVED FROM SIMULATION CALCULATIONS

Al/TiB_2 system

Type 1 and 3 filters

The results shown originated respectively :

1) from the literature (4, 9 and 10), where they derive from laboratory experiments,

and

2) from experiments carried out (11) under conditions more representative of actual industrial practice at Pechiney, as regards filter dimensions and titanium boride concentrations (Figures 8.7, 8.8, and 8.9). Each point plotted is the mean of at least 30 results with a small confidence interval (± 5 %).

Figures 8 call for the following comments :

① The experimental results reported by different investigators can exhibit significant differences. These can arise :

- either from the procedure of introduction of the titanium boride and the mode of dispersion of the seeds,

or from :

- the concentration of titanium boride particles (possible interaction between particles and agglomeration phenomena).

② Despite this, the average level of contact performance determined using the model approximates to the efficiency determined experimentally.

③ An increase in meltvelocity is detrimental and in every case accompanied by a reduction in efficiency.

In conclusion, the experimental results were found on the whole to concord with the predictions of the model, allowing for the assumptions which had to be made on the particle size distribution of the synthetic titanium boride inclusions upstrean and downstrean of the filter.

4. APPLICATION OF MODEL TO COMPARISON OF VARIOUS FILTRATION SYSTEMS

① One immediate application of the process model is in the classification of the initial filtration efficiency of commercially available filters over their recommended range of operating conditions (Table I).

Figure 9 indicates the results obtained under particular conditions of use of filters representative of the three types, DBF, CFF and RMF, and how they vary with particle sizes ranging from 2 to 30 µm for a density of 4.5 g/cm³ (titanium boride).

A point to note is that over the range of melt velocities represented, and which correspond to industrial use of the various types of filters, there were found to be distinct differences in efficiency.

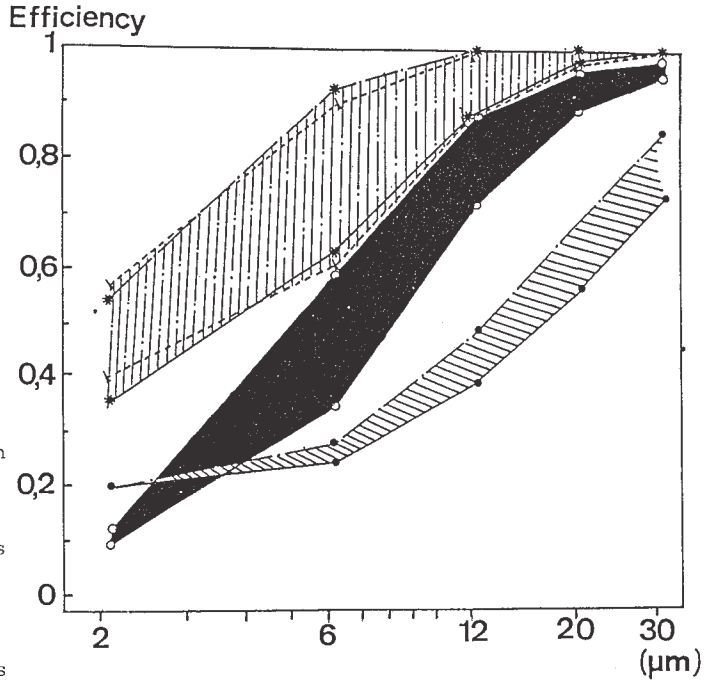

FIGURE 9

USE OF MATHEMATICAL MODEL TO COMPARE VARIOUS FILTRATION PROCESSES

Deep bed of fine (20 cm thick) or coarse (50 cm thick) granulate
Filter cartridge consisting of fine granulate bougies (thickness 2 cm)
Ceramic foam, 40 ppi (tickness 5 cm)

The upper boundary of each hatched region corresponds to the low velocity shown in Table I, while the lower boundary corresponds to the high velocity.

The various types of filters can be classified in order of decreasing efficiency as follows :

- deep bed of fine or coarse particulate material (DBF)
- fine sintered grains featuring high filtration area and low thickness (RMF)
- ceramic foams (CFF) characterised by low thickness and high melt velocity.

② Filter media can also be classified according to their coefficient of filtration (λ_i).

In this case, the coefficient of filtration affords a rigorous comparison of the behaviour of different structures in terms of contact per elementary section. Figure 10 illustrates the variations in maximum filtration coefficient (corresponding to unit probability of retention) for DBF, RMF and CFF filters, again for melt velocities representative of industrial practice except for the last-mentioned.

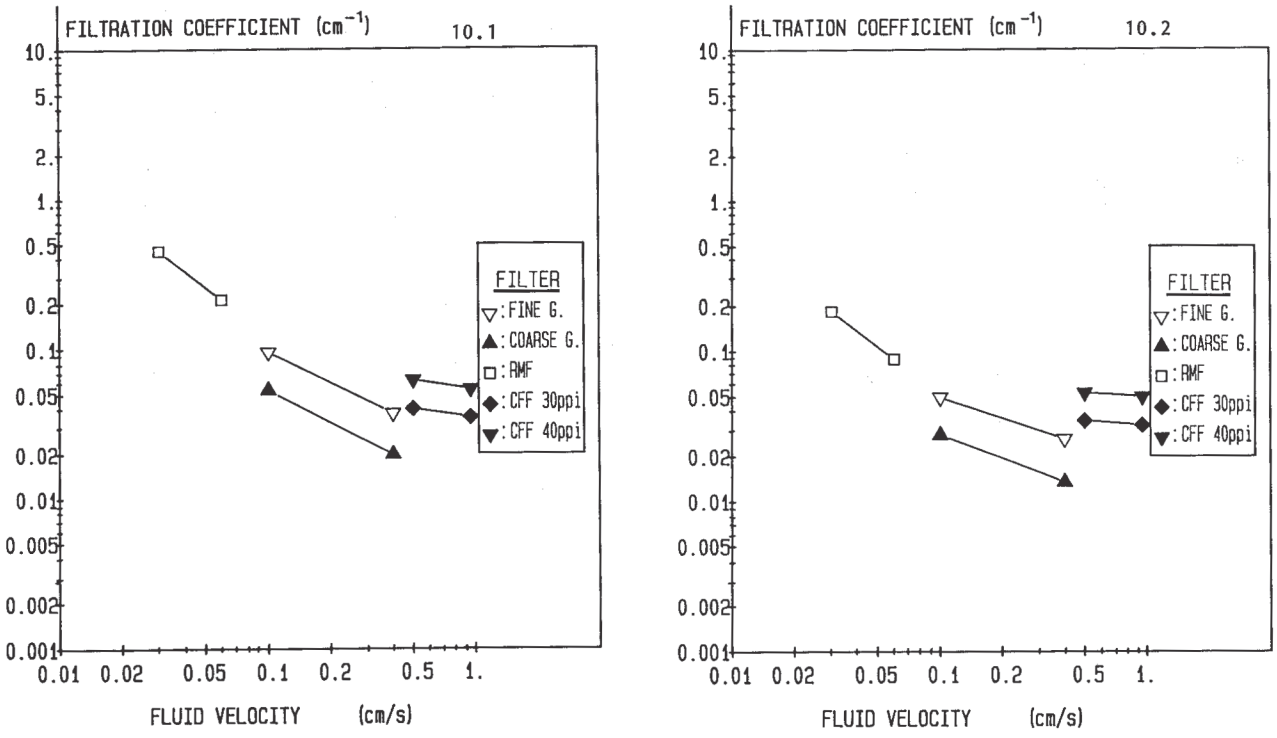

FIGURE 10

MAXIMUM FILTRATION COEFFICIENT FOR DIFFERENT FILTERS
(Cf. Table I) (Particle diameter 6 µm)

10.1 ρ_p = 4.5 g/cm³ 10.2 ρ_p = 3.3 g/cm³

The CFF filters were observed to be less sharply differentiated in terms of the coefficient of filtration λ_i than in terms of probable maximum efficiency (Figure 9). In industrial practice, this type of filter is penalised as regards filtration efficiency, i.e. the retention of fine inclusions, by the thickness of the filter medium (5 cm) and by the range of melt velocities recommended by the makers (0.7 to 1.4 cm/s).

CONCLUSION

An original model (the unit cell pattern) of the operation of deep-bed filters, simulating the retention of inclusions contained in the liquid metal, has been developed, adjusted and put to use.

The model can be employed to estimate the maximum initial efficiency of deep-bed filtration over a wide range of operating conditions.

Bearing in mind the assumptions made in the construction of the model, i.e.

- vertical flow pattern

- an initial probability of retention equal to unity

it is possible to assess the relative effects on probability of contact of parameters as different as melt velocity, filter structure (granular or open-pore), average pore size or the thickness of the filter employed.

As against this, the model makes no allowance for :

- the nature of the filter medium (inert material or flux)

- the surface condition of the filter medium against which the liquid rubs (roughness and microporosity).

Again, it will not predict filter clogging ; it has nothing to say about the progression of the filtration front.

Where macroscopic structures are equivalent, the model will not differentiate media in terms of the microstructure, which determines the number of sites available to trap an retain particulate matter.

Its main advantage is that it makes it possible to determine operating conditions able to guarantee the desired initial efficiency in terms of the removal of a given type of inclusions.

BIBLIOGRAPHY

(1) APELIAN, D ; MUTHARASAN, R ; ROMANOWSKI, CA ; MILLER, R.E and ECKERT, C.E ;
Report of the AIME, 1983, pp 935 to 969.

(2) HERZIG, J.P ; LECLERC, D.M ; LEGOFF, P.
Flow of suspensions through porous media - Application to deep filtration. Industrial and Engineering Chemistry, 1970, (5), pp. 8 - 35.

(3) DELACHAMBRE, Y.
Contribution à l'étude de l'écoulement d'une suspension à travers un milieu poreux et du mécanisme de la filtration.
Thèse - Faculté des Sciences de Nancy, France 1966.

(4) CONTI, C.
Contribution à l'étude de la filtration profonde des métaux.
Thèse de Doctorat - Faculté Polytechnique de Mons, Belgique, 1983.

(5) RAJAGOPALAN, R.J ; TIEN, C.
Progress in filtration and separation.
Ed. Wakeman, Elsevier Publ. Comp., 1979, vol. 1, pp. 180 - 266.

(6) PAYATAKES, A.C ; TIEN, C ; TURIAN, R.M.
a new model for granular porous media - Model formulation.
A.E.Ch.E. Journal, 1973, (1°, pp.58 - 67.)

(7) PAYATAKES, A.C ; TIEN, C ; TURIAN, R.M.
Trajectory calculation of particle deposition in deep bed filtration.
A.I.Ch.E. Journal, 1974, (9), pp. 889 - 905.

(8) CONTI, C ; JACOB, M.
Depth filtration of liquid metals : application of the limiting trajectory method to the calculation of inclusion deposition in open cell structure filters.
Bulletin de la Société Chimique de France, 1984, (11 - 12), pp. 297 - 313.

(9) APELIAN, D.
New developments in aluminium processing - Filtration.
Solidification Processing Conference, Leuven, 1981, Belgium.

(10) APELIAN, D ; MUTHARASAN, R.
Filtration : a melt refining method.
Journal of metals, 1980, (9), pp. 14 - 19.

(11) NETTER, P.
Mesures des performances initiales de filtration de divers milieux poreux.
Rapport interne, 1985 ; Cegedur Pechiney, Voreppe France.

(12) GAUKLER, L.J : WEABER, M.M ; CONTI, C ; JACOB-DULIERE, M.
Industrial application of open pore ceramic foam molten metal filtration.
Report of the A.I.M.E. Meeting, 1985, New York U.S.A.